AIAA JOURNAL
Vol. 33, No. 11, November 1995

Quantification of Aero-Optical Phase Distortion Using the Small-Aperture Beam Technique

Eric J. Jumper* and Ronald J. Hugo†
University of Notre Dame, Notre Dame, Indiana 46556

This paper discusses the small-aperture beam technique, a new way of experimentally quantifying the instantaneous optical wave front distortions imposed by propagation through an optically active, turbulent flowfield. The paper lays out the theoretical basis for the technique and the relationship of the measured jitter of a small-aperture probe beam to optical path difference. A numerical simulation of a two-dimensional heated jet is used to explore the validity of using beam-jitter signals from multiple probe beams to obtain optical path difference in a flow region where eddy production constitutes the major character of the "turbulent" flowfield.

I. Introduction

WHEN an otherwise collimated beam of light is made to propagate through an aberrating index-of-refraction field, the wave front becomes distorted. Depending on the spatial frequencies/wavelengths of the distorted wave front and the aperture (diameter) of the beam, the wave front distortion affects the beam's ability to be focused and directed. As such, aberrating index-of-refraction fields detract from the primary objective of an optical system that might include a bore-site error and/or a centroid error in the case of a tracking system, a blur and identification problem in the case of an imaging system, or a reduction in (time-averaged) intensity on target both by defocus and jitter in the case of a directed energy (laser) weapon system, for example. If the aberrating index-of-refraction field is due to a turbulent flow (i.e., turbulent boundary layer, shear layer, or wake, for example) the problem is further complicated by the fact that the field is temporally dynamic.

The optical/turbulent-fluid interaction problem is hardly a new area of concern; analytical studies considering the propagation of radio waves through the atmosphere were performed as early as 1950,[1] while the propagation of light through a compressible turbulent boundary layer was investigated analytically in 1952[2] and experimentally in 1956.[3] The specific problem of propagation of light through a turbulent flowfield received a burst of activity starting in the late 1960s[4] and peaked with the publication of Ref. 5. All of this work concentrated on describing the fluid-optical interaction in terms of a statistical process.

Such a statistical representation of both the wave front aberration and the turbulence was not only justified but also the only practical approach since, until fairly recently, the study of turbulence itself focused on describing the statistics of the turbulent flowfield. Such statistical descriptions contain mean velocity and temperature profiles, rms fluctuations of these quantities, and power spectral density (PSD) functions for the frequency content of the fluctuations. These descriptions have been useful in building models of the turbulence for the purpose of predicting average velocity and temperature fields, shear stress at surfaces, pressure distributions, heat transfer, etc. The models have also been somewhat successful in describing time-averaged mixing, i.e., mean concentration profiles.

For the most part, the aforementioned fluid-optical interaction studies[5] have focused on characterizing the flowfield in terms of hot-wire measurements processed in the usual statistical manner just described, as well as some measure of correlation length for density fluctuations as a function of position along the intended optical propagation direction; the optical-phase "degradation" was then characterized by means of one or a limited number of interferograms (generally double-pulsed) or by looking at the far-field, time-averaged (in some sense) focus. These characterizations of the flowfield and the optical phase distortion were then used to compare to each other by means of linking equations derived for "statistical" flowfields. The most commonly used linking equation is that for the optical path variance,[6] σ^2, given certain measured properties of the flowfield

$$\sigma^2 = 2G^2 \int_0^L \sigma_{\rho'}^2 \Lambda_{\rho'} \mathrm{d}z \tag{1}$$

where G is the Gladstone–Dale constant of the medium, $\sigma_{\rho'}^2$ is the variance of the density fluctuation at a specific location in the flow normal to the propagation path, and $\Lambda_{\rho'}$ is the integral length scale of the density fluctuations. Evaluation of $\Lambda_{\rho'}$ in Eq. (1) requires either a direct measurement or an assumption of a specific turbulence statistical distribution for the covariance of the density fluctuations.

In the end, such studies were able to verify that, given the turbulent-flow statistics, the linking equations between the fluid mechanics and optical degradation predicted the approximate magnitude of the time-averaged optical degradation in the far field.[5,7–9] Unfortunately, these methods gave only an approximate feel for the extent of the optical degradation; they could not make the link between the fluid mechanics and a continuous time history of the instantaneous optical phase front as it emerged from the turbulent flow. Yet information of this sort is of crucial importance for the successful application of adaptive-optical corrections[10] to optical systems transmitting through aero-optical flowfields.

More recent aero-optical studies have recognized the importance of the structure of turbulence to the study of the aero-optical problem. Reference 11, for example, recognized the importance of exposure time in characterizing the far-field intensity profile and was able to link this characterization to the coherent structures in a shear layer. Reference 12 specifically addressed the structure of turbulence in numerical studies that used direct numerical simulation results; however, these studies addressed only a handful of single instantaneous realizations.

In this paper, we attempt to address the question of how aero-optical data might be taken and interpreted in a way that is both more meaningful to optical system designers and efficient to collect. The word "meaningful" is interpreted to mean that a measurement of the instantaneous spatial and temporal optical wave front is important. Interferograms have long been used to capture the instantaneous (snapshot) spatial wave front distortion, but the number and acquisition rate of interferograms needed to provide temporal histories of the distortion are prohibitive. As was pointed out

Presented as Paper 92-3020 at the AIAA 23rd Plasmadynamics and Lasers Conference, Nashville, TN, July 6–8, 1992; received Sept. 25, 1993; revision received April 18, 1995; accepted for publication May 1, 1995.

*Associate Professor, Department of Aerospace and Mechanical Engineering. Associate Fellow AIAA.

†Graduate Assistant, Department of Aerospace and Mechanical Engineering. Member AIAA.

during the recent presentation of Ref. 9, at the Aerospace Sciences Meeting,[13] 10 interferograms were used to attempt to extract statistical rms phase-front distortion for a compressible shear layer experiment; the experimenters stated that at least 10 times and perhaps as much as 100 times this number of interferograms would be needed to extract reliable rms phase-distortion information. Further, the instantaneous spatial wave front distortion measured by interferometry consists of discrete snapshots taken at nonconsecutive instants in time. As such, it is not sufficient to address the question of what aero-optical data might be taken that is meaningful without adding the requirement that the collection of meaningful data must also be efficient to be useful.

Very recently a new technique for obtaining statistical spatial and temporal optical distortion information efficiently was developed by Malley et al.[14] that made use of a small-diameter (small-aperture) laser beam directed through the aberrating flowfield. The off-axis displacement was measured by a rapid-response detector and converted to off-axis angle, a time series of which was used to infer the rms optical distortion. By various Fourier techniques, information from this single beam could be used to characterize the spatial scale and temporal frequency of the optical distortion that would be imposed on an optical wave front traversing the flowfield along a path parallel to the path of the small-aperture probe beam. This method was shown to give results compatible with rms optical distortion inferred from a large number of interferograms, yet the method allowed the collection and processing of the information in a much more efficient manner than that required using interferometric methods. At almost the same time, Wissler and Roshko[15] investigated the time histories of a small-aperture beam propagated through a plane shear layer in much the same way that was used in Ref. 14 but studied the instant-to-instant characteristics of the beam's deflection. By analyzing the time histories, they were able to associate specific characteristics of the beam's deflection with specific flowfield structures in the shear layer. These two techniques hinted at the possibility of capturing not only a statistical characterization of the optical distortion but also more detailed information about the instant-to-instant wave front distortion over a large viewing aperture. In our work, we have made use of multiple small-aperture probe beams to capture this more detailed information about the time history of a rapidly distorting optical wave front as it emerges from an aberrating turbulent flowfield; we term this capture technique the "small-aperture beam technique." This paper describes the theory behind the technique and demonstrates its potential in capturing a time series of instantaneous wave fronts by applying the method to a computed two-dimensional shear-layer flowfield.

II. Small-Aperture Beam Technique

The small-aperture beam technique (SABT) involves collecting a time history of the off-axis movement of a small-diameter (aperture) laser beam as it traverses an optically active flow. We will refer here to the small-aperture beam as the probe beam, and it is assumed that its diameter is much smaller than the dimension of a larger aperture beam intended to traverse the same flow, and whose optical distortion character is of interest. The information extractable from the probe beam's time history follows directly from the theory of geometric optics.

Geometric optics is based on Huygen's principle,[16] from which it is known that a ray of light is always normal to the optical wave front. The unit vector in the direction of the ray is given by the so-called ray-tracing equation

$$\frac{\mathrm{d}}{\mathrm{d}s}(n\hat{\tau}) = \nabla n \tag{2}$$

where $\hat{\tau}$ is the propagation-direction unit vector, n is the index of refraction of the medium in which the light travels, and s is the propagation distance.[16]

If a small-aperture beam is used to probe an aberrating medium [i.e., $n = n(x, y, z, t)$], then the direction of the path that it will follow is given by Eq. (2), assuming that the spatial scales of the phase distortion of a larger aperture beam traversing the same aberrating medium are large compared with the diameter of the small-aperture

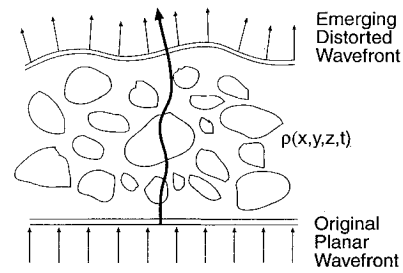

Fig. 1 Wave front distortion and probe beam.

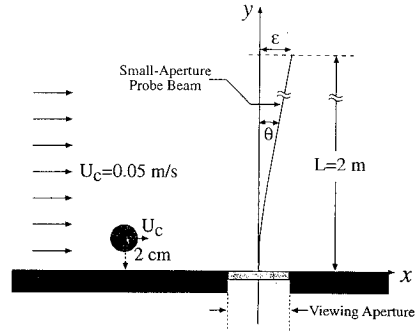

Fig. 2 Turbule dynamics.

probe beam, i.e., $a/\Lambda \ll 1$ where a is the diameter of the small-aperture probe beam and Λ is the integral length scale of the optically active structures.

Figure 1 shows a schematic of an initially planar wave emerging from a turbulent aberrating medium. The subsequent emerging wave front is thus distorted. This distortion is usually quantified as either an optical path length (OPL) or as an optical path difference (OPD). Optical path length is defined as[16]

$$\mathrm{OPL} = \int_{s(A)}^{s(B)} n\,\mathrm{d}s \tag{3}$$

where n is the index of refraction, and $s(A)$ and $s(B)$ refer to positions along the direction of optical propagation. OPD is the local difference between the optical path length at a given location and the average optical path length over the aperture. The presence of nonzero OPD over an aperture is, in fact, what an instantaneous or pulsed-laser interferogram measures directly at a given instant in time. The OPD and the optical wave front distortion (shown on the emerging wave front in Fig. 1) are related by being conjugates to one another for the case of propagation through air.

Also shown in Fig. 1 is a single probe beam as it traverses the medium (note that the path and the distorted wave front are greatly exaggerated). Its path direction changes continuously along the traverse, but as it emerges, it is normal to the local wave front. Thus, the small-aperture beam technique is able to capture a time history of the spatial derivative of the wave front at a probe beam location.

Relation Between Probe Beam Time History and Optical Wave Front Distortion

Consider first, a single temperature perturbation convecting through the probe beam path. For simplicity, we choose to consider here only a two-dimensional flow perturbation. This single perturbation might be thought of as due to a single turbulent eddy (turbule) convecting through the beam. As an example, consider a turbule described by a Gaussian distribution given by

$$T'(x, y) = 10\exp[-160{,}000(x^2 + y^2)]\,\mathrm{K} \tag{4}$$

The path of the eddy is shown schematically in Fig. 2. The jitter time history that would be produced by the small-aperture probe beam as the turbule convects by is shown in Fig. 3, as computed using Eq. (2). Since the convection velocity, U_c, is $\mathrm{d}x/\mathrm{d}t$ and $\theta(t, x = 0)$

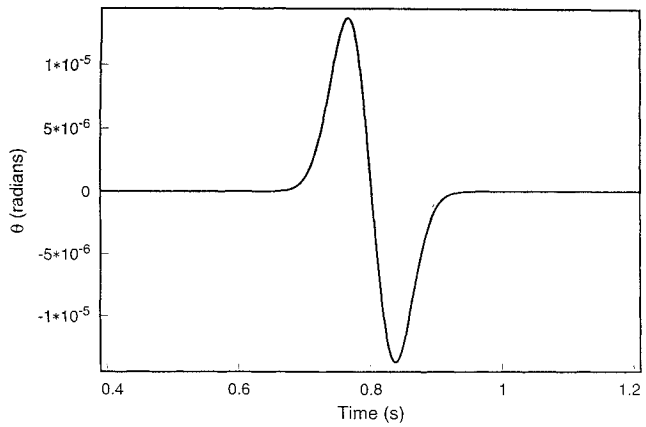

Fig. 3 Time history of beam jitter.

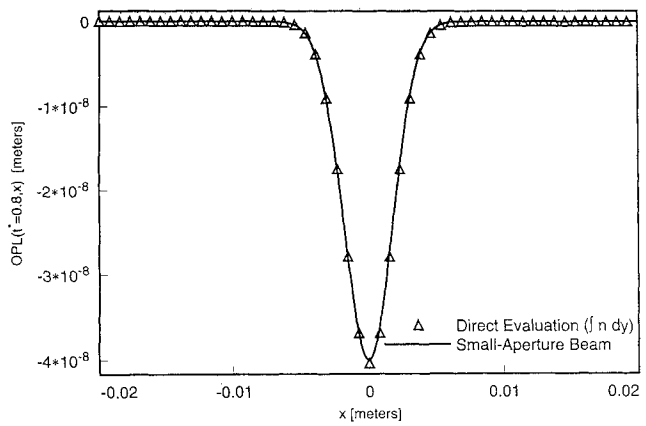

Fig. 4 Resulting optical path length.

is $[-\mathrm{dOPL}(t, x)/\mathrm{d}x]|_{x=0}$, the optical path length referenced to the undisturbed beam is given by

$$\mathrm{OPL}(t, x = 0) = \int_{t_0}^{t} -\theta(t, x = 0) U_c \, \mathrm{d}t + \mathrm{OPL}(t_0, x = 0) \quad (5)$$

The negative sign in front of $\theta(t, x = 0)$ in Eq. (5) results from the fact that the OPL and the optical wave front are conjugates.

Equation 5 yields the optical path length at the location of the small-aperture beam ($x = 0$), as a function of time. To obtain the optical wave front both as a function of space (across the aperture) and time, Taylor's frozen-flow hypothesis[17] and the following equation can be used:

$$x = -U_c(t - t^*) \quad (6)$$

where t^* refers to the instant in time at which the spatial OPL is desired. When Eqs. (5) and (6) are applied to the convecting turbule problem [with $\mathrm{OPL}(t_0, x = 0) = 0$], the optical path length as a function of space can be computed for a specific time t^*. For the case of $t^* = 0.8$ s, the resulting OPL is as shown in Fig. 4. It is noted that at $t^* = 0.8$ s the center of the convecting turbule is located at spatial location $x = 0$. Also shown in Fig. 4 is the optical path length evaluated directly by integrating the following equation:

$$\mathrm{OPL}(t^* = 0.8, x) = \int_0^L n(t^* = 0.8, x, y) \, \mathrm{d}y \quad (7)$$

The maximum error in OPL between the small-aperture beam approach [Eqs. (5) and (6)] and the direct evaluation approach [Eq. (7)] is 1.02% and occurs at $x = 0$. It should be noted that as close as the agreement is, it can be made even closer by sampling $\theta(t)$ more often, thereby increasing the spatial resolution. This is an important result because it demonstrates that, for a flowfield in which Taylor's frozen-flow hypothesis holds, the information provided by only a single probe beam is capable of measuring the instantaneous spatial and temporal optical wave front. The ramifications of applying the methods to a flowfield in which Taylor's frozen-flow hypothesis does not hold will be discussed in the next section.

The information contained in the beam-jitter signal can also be used to obtain statistical quantities for the optical degradation, as was demonstrated in Ref. 14. From a time series of the probe beam's position the mean bore-sight error (BSE) can be calculated as

$$\overline{\mathrm{BSE}} = \frac{1}{N} \sum_{i=1}^{N} \theta_i \quad (8)$$

where θ_i is the digitized off-axis beam angle at time t_i, and N is the number of samples in the time series. Further, the variance of the BSE can be immediately obtained as

$$\overline{\mathrm{BSE}^2} = \frac{1}{N} \sum_{i=1}^{N} (\theta_i - \bar{\theta})^2 \quad (9)$$

It should be pointed out that no assumption need be made concerning convection velocity to compute BSE information; however, a convection velocity must be assumed or otherwise determined to infer information about OPD. Since $\theta = -\mathrm{dOPL}/\mathrm{d}x$, the optical path length at some time t_j is given as

$$\mathrm{OPL}(t_j) = \int_{t_0}^{t_j} \theta \frac{\mathrm{d}x}{\mathrm{d}t} \, \mathrm{d}t \quad (10)$$

Given an appropriate convection velocity U_c (i.e., values for U_c from the literature are usually taken as $0.6U_{\text{centerline}}$ for a two-dimensional jet, $0.8U_\infty$ for a boundary layer, or $\bar{U}$ for a free shear layer, for example), $\mathrm{d}x/\mathrm{d}t = U_c$ allows one to write

$$\mathrm{OPL}(t_j) = \int_{t_0}^{t_j} \theta U_c \, \mathrm{d}t \quad (11)$$

which can be discretized as

$$\mathrm{OPL}_j = \mathrm{OPL}(N \Delta t) = \sum_{i=1}^{N} \theta_i U_c \Delta t \quad (12)$$

The mean optical path length is just

$$\overline{\mathrm{OPL}} = \frac{1}{N} \sum_{j=1}^{N} \mathrm{OPL}_j \quad (13)$$

from which one can obtain the rms OPD as

$$\mathrm{OPD}_{\mathrm{rms}} = \sqrt{\frac{1}{N} \sum_{j=1}^{N} (\mathrm{OPL}_j - \overline{\mathrm{OPL}})^2} \quad (14)$$

Thus, having only the data from a single probe beam along with a convection speed allows one to obtain as much information about the phase error as all of the previous, and often laborious, methods that have gone before. This result was demonstrated in Ref. 14 where the information from a single probe beam was used to infer statistical optical degradation ($\mathrm{OPD}_{\mathrm{rms}}$) values using Fourier analysis techniques. The small-aperture beam technique is, however, capable of measuring far more than just statistical values, as was demonstrated earlier in this section for the convecting turbule problem. To further demonstrate the potential of the small-aperture beam technique, the next section will discuss the application of the small-aperture beam technique to flowfields for which Taylor's frozen-flow hypothesis does not hold.

III. Exploring Validity of Relationship Between Beam Jitter and OPD

It is clear from the previous section that the small-aperture beam technique (SABT) contains the potential for investigating aero-optical phenomena in more detail than has previously been possible; however, much of its exploitation depends on being able to define a "convection velocity" appropriate for using a Taylor's frozen-flow extension of the time series to a spatial description. From our perspective, the extent to which the use of a common convection velocity might be appropriate depends on the relationship between the rate of production of "eddies" or evolution of the turbulent field and the rate at which eddies are convected. If the structure is fully formed, regardless of its complexity, and simply convects, changing little in the time to convect through a region of interest, then the OPD predicted by even a single probe beam should be quite meaningful. If, on the other hand, the turbulent field is evolving at a rate comparable to the convection rate, a predicted OPD would not be expected to resemble actual realizations of the OPD; however, multiple probe beams can be used to capture even this sort of OPD.

To examine the use of multiple probe beams to describe a rapidly evolving "turbulent" flowfield OPD, we have examined a two-dimensional jet in the region from the nozzle exit to a downstream distance of $X/D = 4$, where X is the downstream distance and D is the nozzle exit width. It is well known that the flow is still fairly two dimensional in this region, and this is the region where vortices form and pair at rates comparable to convection rates.[18]

Our approach has been to perform both numerical and physical experiments in this region of a two-dimensional jet ($1.0 < X/D < 4.0$); however, only the numerical studies are given here. To model the flowfield, we used a reduced-model representation similar to that of Acton[19] for an axisymmetric jet. The fluid (air) was made optically active by having the jet hotter than the ambient air.

Numerical Model

The flow was modeled using a discrete-vortex method.[19] The method is inviscid, although a viscous, rotational core was used to avoid the singularity at vortex centers. Each vortex in the field convected at the velocity imposed by all others in the field via repeated application of the Biot–Savart law. The nozzle was modeled by placing rows of 100 discrete vortices for six nozzle widths on both the upper and lower walls of a constant width duct. These vortices remained fixed with time, but one vortex was placed a distance of $(U_j/2)\Delta t$ (where U_j is the jet centerline velocity and Δt is the time step size) just downstream of the nozzle exit, in the downstream direction at each time step. This and all other free vortices were then free to convect as time progressed. To preserve definition in the vortex trajectories, vortices were added between free vortices after a spacing limit was exceeded.[20] These added vortices had strength equal to one-third the sum of that of the adjacent free vortices, and these adjacent vortices were reduced in strength to two-thirds their original strength so that the net circulation was preserved.

The absence of the inclusion of viscosity in the model is justified on at least two counts. First, at this stage in the development of a real flow, small-scale turbulence has not yet formed, and thus only the large-eddy motions are present and these are known to be essentially inviscid.[21] Second, we are interested only in capturing the character of a flow similar to that of a real two-dimensional jet and are not attempting to simulate the flow exactly. The absence of viscosity is mirrored in our treatment of the temperature field; no molecular diffusion is taken into account, nor is the temperature allowed to influence the flowfield. The fluid is assumed to be either hot or cold, depending on which side of a dividing line it lies, the dividing line being defined by the convecting vortices. In the numerical simulation, the ambient temperature T_∞ was set to 22°C and the jet temperature T_j to 76°C. Optical information was extracted as the flowfield evolved by computing actual instantaneous OPDs directly, along with continuous probe beam jitter signals from five downstream locations ($X/D = 2.0$, 2.4, 2.8, 3.2, and 3.6).

Flowfield Numerical Results

Figure 5 shows a typical flowfield representation and a flow visualization of a two-dimensional jet experiment[22]; the essential

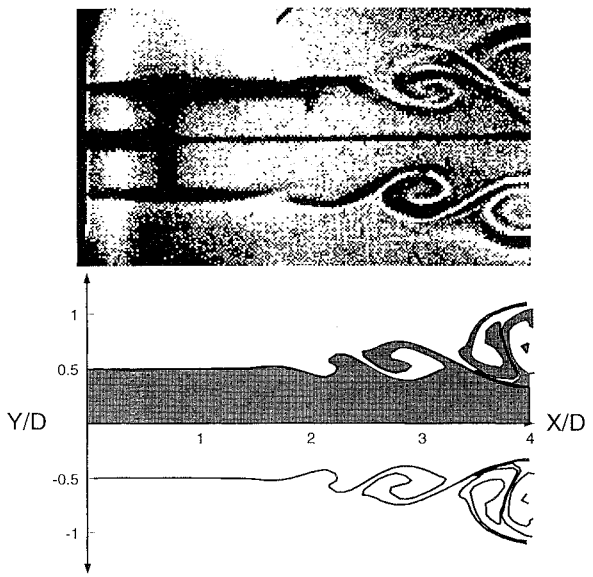

Fig. 5 Experimental (top—Ref. 22) and numerical (bottom) flowfields.

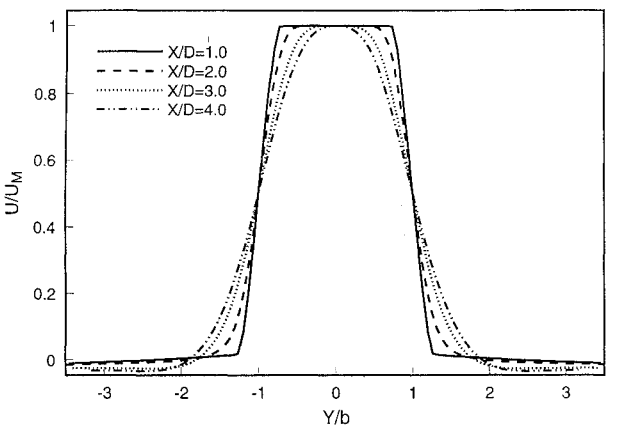

Fig. 6 Time-averaged velocity profile at various downstream locations.

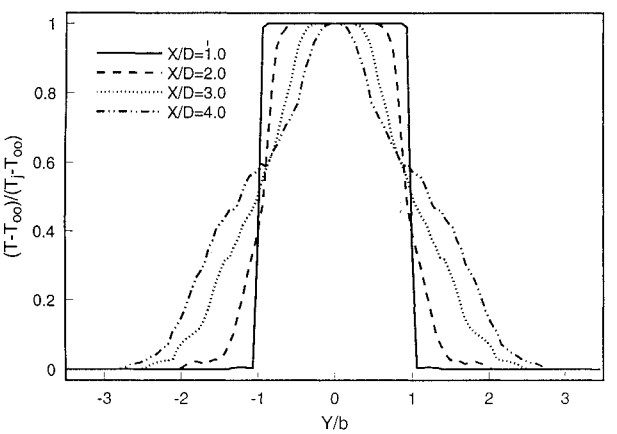

Fig. 7 Time-averaged temperature profile at various downstream locations.

character of the experimental flow appears to be captured by the numerical flow. The darkened region of the numerical flow represents the hot fluid. Time-averaged velocity and temperature fields were constructed from time series of instantaneous representations of the velocity and temperature field. Figures 6 and 7 show the time-averaged velocity and temperature fields at X/D locations of 1.0, 2.0, 3.0, and 4.0, based on the average velocity and temperature histories. In both figures the flowfield locations have been nondimensionalized by the jet half width b that denotes the Y location at which the velocity is 50% the local centerline value. Although

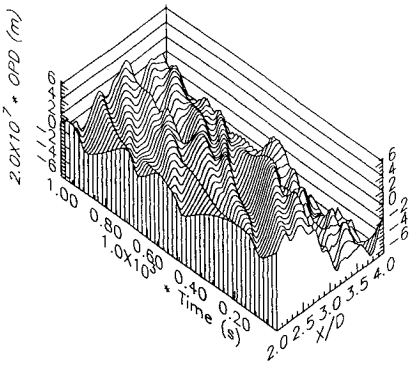

Fig. 8 Waterfall plot of OPDs.

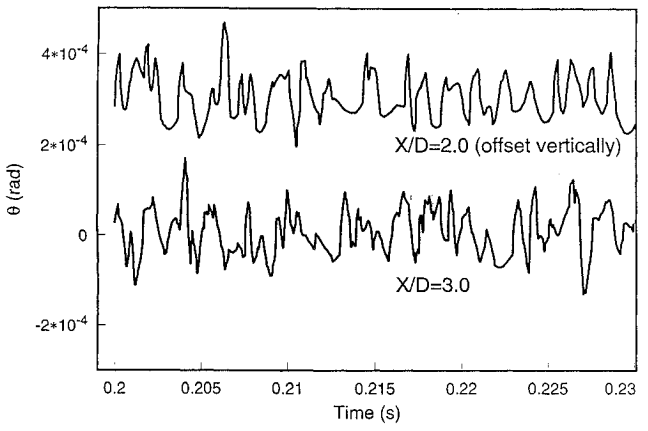

Fig. 9 Jitter time series.

instantaneous velocity fields look quite chaotic, they are continuous since the velocity field itself is continuous (i.e., constructed from repeated applications of the Biot–Savart law over the entire set of vortices); in turn, its averaged properties are smooth and agree with time-averaged experimental data.[22,23] The temperature profiles also agree with those from experiments,[22,23] to the point of even demonstrating a similar inflectional point in the profiles (at $Y/b = 1.0$) for locations downstream of $X/D = 2.0$.

Optical Numerical Results

Based on the preceding comparisons with experiment, we felt justified in using the numerically produced optical data to begin to address and infer the nature of the relationship between the jitter signal and the OPD. To begin with, Fig. 8 shows a series of successive (in time) actual OPDs for the region from $X/D = 2.0$ to 4.0. It can be seen that the OPDs do appear to convect. As time advances, the fidelity of the convecting OPD begins to erode. Even so, it is possible to infer some information from these OPDs. First, consider the rate at which the structures convect. Tracking individual structures (as best we could determine them) showed that the structures convected at rates that varied from roughly one-fourth the jet exit velocity to approximately 90% the jet exit velocity; however, on average, the range was from approximately half to approximately 75% the jet exit velocity over the region from $X/D = 2.0$ to 4.0.

Jitter time series were also produced at five X/D locations, 2.0, 2.4, 2.8, 3.2, and 3.6; sample jitter data are shown in Fig. 9. The fact that the flowfield is evolving rapidly is evidenced in the increasing complexity of the jitter signal as the streamwise location increases. At face value, this might suggest that attempted constructions of OPDs might bare little resemblance to the actual OPDs. Using these jitter signals and the average convection velocity at each location, predicted OPDs were made for several times and compared with the actual instantaneous OPD for that time. Figures 10 and 11 show a typical set of predicted OPDs along with the actual OPD, and the arrows at the bottom of each figure denote the locations of the probe beams. As expected from the increasing complexity of the jitter signals with X/D location, in general the agreement between the

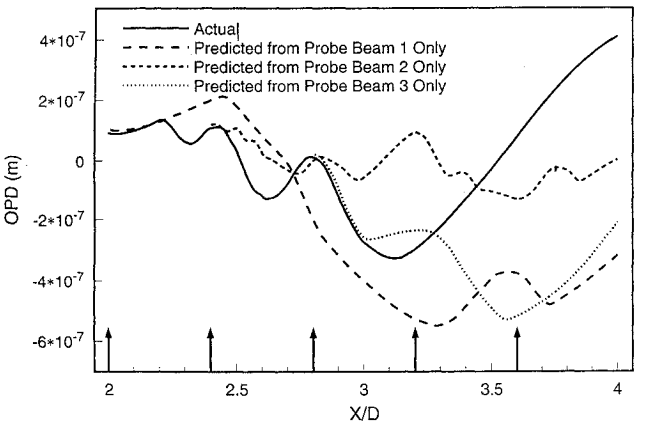

Fig. 10 Actual and predicted OPDs using probe beams 1, 2, and 3.

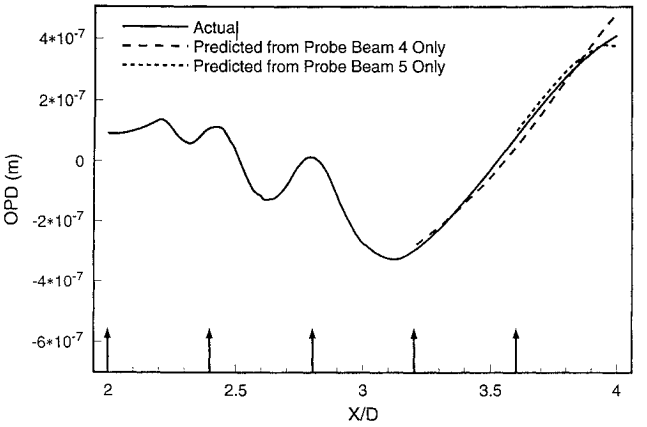

Fig. 11 Actual and predicted OPDs using probe beams 4 and 5.

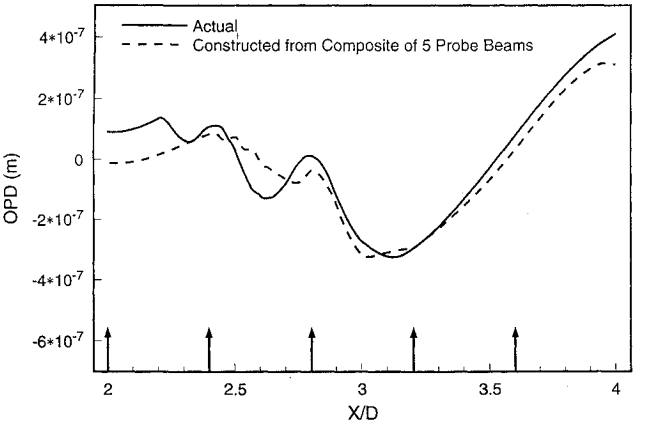

Fig. 12 Actual and composite predicted OPDs.

predicted and actual OPDs is poor; however, it should be noticed that the OPD predicted by each probe beam jitter series is similar to the actual OPD just downstream of its own location.

The implication of the preceding observation appears to be that, in general, there exists a limited distance over which the beam jitter is able to produce a close approximation to the actual OPD; this distance and the desired accuracy of the approximation form a criteria for how many probe beams are needed to describe the optical distortion. With this in mind, we constructed composite OPDs at various times from the five probe beam jitter signals in such a way that each probe constructed the OPD over a distance from itself to the next probe; Fig. 12 is one of these composites.

In comparing the two OPDs of Fig. 12, it should be kept in mind that the constructions depend on knowing a convection speed, and the magnitudes of the constructed OPDs will be sensitive to errors in estimating or otherwise obtaining these speeds. This disclaimer

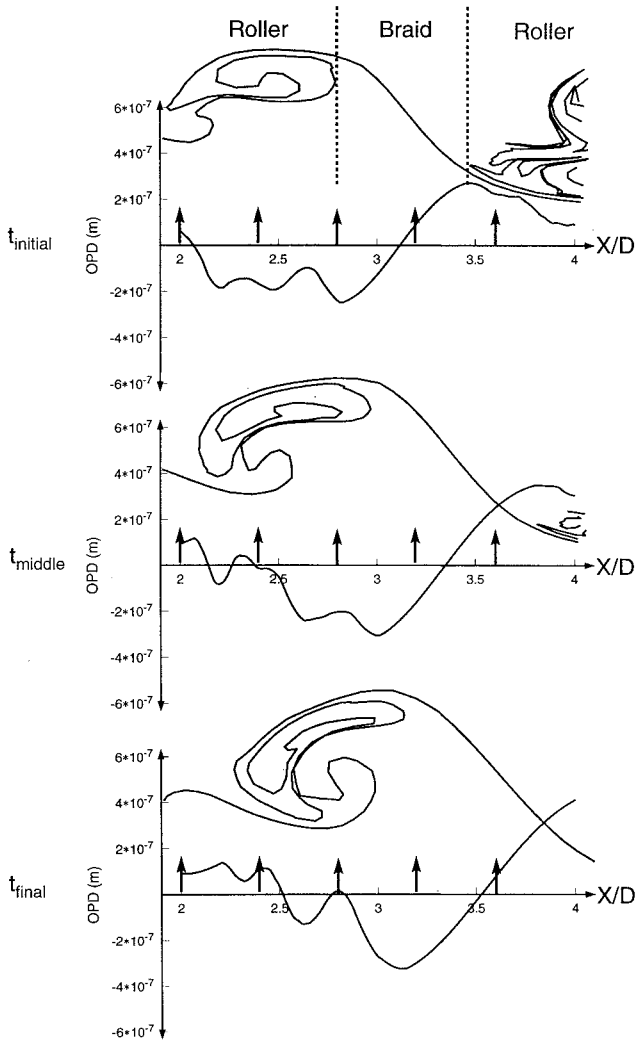

Fig. 13 Flowfield and OPD evolution during period of composite OPD construction.

aside, the construction, although not perfect, is remarkably similar to the actual OPD. Inferences about the spatial and the temporal character of the OPD obtained from such a sparse "instrumentation" array would be close to those of the actual, time-evolving OPD.

It is of note that the constructions are as faithful as they are even though they represent OPDs from a rapidly evolving region of the flowfield. To impress this point more strongly, a series of three realizations of the flowfield and its concomitant OPDs are given in ascending order with time in Fig. 13. The top-most realization corresponds roughly to the flow at the time the probe beams would begin a stream of data that would result in the final construction given previously in Fig. 12; the middle corresponds roughly to the point at which approximately half of the jitter data for the construction would have been accumulated; and the bottom realization is the last realization and the one that corresponds to the point in time that the construction is formed. The arrows in Fig. 13 indicate the locations of the five probe beams. It is clear that the flow structure evolves over this interval, and yet even some of the high-spatial-frequency detail is preserved in the constructed OPD.

Figure 13 also reveals the relationship between the shear layer's roller-braid combination and the resulting OPD as noted in Ref. 15. Note that the roller-braid combination produces an optical degradation with the smallest spatial frequency, whereas the detailed structure inside of the roller is seen to produce optical degradations with the highest spatial frequencies.

The overall error between the actual OPDs and the constructed OPDs was evaluated by computing the root-mean-square error between the constructed OPD and the actual OPD. The root-mean-square error was evaluated over 256 evenly spaced points over the viewing aperture ($X/D = 2.0 \rightarrow 4.0$) for 150 time steps of the numerical simulation, representing a flow convection distance of approximately 17 nozzle widths. The choice of 150 time steps for the evaluation of the root-mean-square error was made after it was found that the magnitude of the error changed very little with a further increase in the number of time steps. The root-mean-square error is evaluated by

$$\text{rms OPD error} = \sqrt{\frac{1}{150 * 256}\sum_{i=1}^{256}\sum_{j=1}^{150}[\text{SABT OPD}(x_i, t_j) - \text{Actual OPD}(x_i, t_j)]^2} \tag{15}$$

Using Eq. (15), the rms OPD error was computed to be 1.348×10^{-7} m, for a peak-to-peak OPD of 5.0×10^{-7} m, leading to an error of approximately 27% (based on the peak-to-peak OPD).

IV. Conclusions

In this paper we have introduced a sparse-instrument method (the small-aperture beam technique or SABT) of measuring the optical wave front distortions due to the propagation of a large-aperture, collimated laser beam through an aberrating, turbulent flowfield. The purpose of this paper has been to describe the physics behind the method. The method takes advantage of the fact that the structures on the wave front convect through the viewing aperture, as the aberrating fluid structures convect with the flowfield. The basis of the method was described both through a simple, ideal model problem and through wave front constructions for propagation through a numerically simulated, highly evolving two-dimensional heated jet. In the latter case, the wave front construction was made using the jitter signal from each of five probe beams to construct the wave front from one probe beam to the next using only the jitter time history from the upstream probe beam. This is, in fact, the crudest method of constructing the wave front from the information available from, in this case, the five probe beams; with this method, the rms error in constructing the instant-to-instant wave fronts was 27%. Examination of individual wave fronts shows that, although this error is present, the spatial character of the wave fronts is preserved on an instant-to-instant basis. An SABT instrument, using even this crude wave front construction technique, could provide details about the time-evolving character of aero-optical wave front distortion that has not previously been available for study by other methods. Even with the 27% error demonstrated here, it would be possible to extract detailed information about the instant-to-instant far-field patterns of an initially collimated, large-aperture laser beam that might be directed through the flowfield; using statistical information inferred about the wave front using previous methods, only crude approximations of the far-field pattern statistical, time-averaged degradation could be estimated. Having the instant-to-instant character of the wave front provided by the SABT would allow for detailed studies assessing the design requirements for an adaptive-optical system and its predicted effect on the far-field patterns.[24]

Although these kinds of studies are possible with the 27% error reported here, other techniques have been explored for combining jitter signals to construct wave fronts between probe beams.[25] Using one of the optimized techniques for the numerically simulated heated jet, the accuracy of the constructions could be improved to an error of approximately 20%; if the number of probe beams were doubled (from 5 to 10 probe beams) and the optimized technique applied, the error could be improved to less than 10%.[24] For measurements on an actual heated jet with the same jet core temperatures and velocities, because the experimental jet evolves more slowly than the numerical simulation, wave front constructions with errors of less than 6% and 2% can be realized using the 5- and 10-probe beam versions of the SABT, respectively.[24]

Acknowledgments

This work was sponsored by the Air Force Office of Scientific Research under the technical management of James McMichael, Grant F49620-93-1-0163, and by a grant from the Phillips Laboratory under the technical management of John Wissler. Finally, the

authors were saddened to hear of the death of Michael M. Malley; his early contributions to the use of small-aperture probe beams for the assessment of aero-optical effects are both acknowledged and appreciated. His creativity and contributions to the community will be greatly missed.

References

[1]Booker, H. G., and Gordon, W. E., "A Theory of Radio Scattering in the Troposphere," *Proceedings of the IRE*, Vol. 38, No. 4, 1950, pp. 401–412.

[2]Liepmann, H. W., "Deflection and Diffusion of a Light Ray Passing Through a Boundary Layer," Douglas Aircraft Co., Santa Monica Div., Douglas Rept. SM-14397, Santa Monica, CA, May 1952.

[3]Stine, H. A., and Winovich, W., "Light Diffusion Through High-Speed Turbulent Boundary Layers," NACA RM A56B21, May 1956.

[4]Sutton, G. W., "Effect of Turbulent Fluctuations in an Optically Active Fluid Medium," *AIAA Journal*, Vol. 7, No. 9, 1969, pp. 1737–1743.

[5]Gilbert, K. G., and Otten, L. J. (eds.), *Aero-Optical Phenomena*, Vol. 80, Progress in Astronautics and Aeronautics, AIAA, New York, 1982.

[6]Steinmetz, W. J., "Second Moments of Optical Degradation Due to a Thin Turbulent Layer," *Aero-Optical Phenomena*, edited by K. G. Gilbert and L. J. Otten, Vol. 80, Progress in Astronautics and Aeronautics, AIAA, New York, 1982, pp. 78–100.

[7]Smith, R., Truman, C., and Masson, B., "Prediction of Optical Phase Degradation Using a Turbulent Transport Equation for the Variance of Index-of-Refraction Fluctuations," AIAA Paper 90-0250, Jan. 1990.

[8]Hogge, C. B., Butts, R. R., and Burlakoff, M., "Characteristics of Phase-Aberrated Nondiffraction-Limited Laser Beams," *Applied Optics*, Vol. 13, 1974, pp. 1065–1070.

[9]Havener, G., and Stepanek, C., "Aero-Optics Testing Capabilities at AEDC," AIAA Paper 92-0760, Jan. 1992.

[10]Tyson, R. K., *Principles of Adaptive Optics*, Academic, San Diego, CA, 1991.

[11]Chew, L., and Christiansen, W., "Coherent Structure Effects on Optical Performance of Plane Shear Layers," *AIAA Journal*, Vol. 29, No. 1, 1991, pp. 76–80.

[12]Truman, C. R., and Lee, M. J., "Effects of Organized Turbulence Structures on the Phase Distortion in a Coherent Optical Beam Propagating Through a Turbulent Shear Flow," *Physics of Fluids A*, Vol. 2, No. 5, 1990, pp. 851–857.

[13]Clark, R., Kalin, D., and Roger, R., Teledyne Brown Engineering, Inc., oral presentation given in conjunction with preceding Ref. 9, Jan. 1992.

[14]Malley, M., Sutton, G. W., and Kincheloe, N., "Beam-Jitter Measurements of Turbulent Aero-Optical Path Differences," *Applied Optics*, Vol. 31, No. 22, 1992, pp. 4440–4443.

[15]Wissler, J. B., and Roshko, A., "Transmission of Thin Light Beams Through Turbulent Mixing Layers," AIAA Paper 92-0658, Jan. 1992.

[16]Klein, M. V., *Optics*, Wiley, New York, 1970.

[17]Hinze, J. O., *Turbulence*, 2nd ed., McGraw–Hill Classic Textbook Reissue, New York, 1975.

[18]Thomas, F. O., "Structure of Mixing Layers and Jets," *Applied Mechanics Reviews*, Vol. 44, No. 3, 1991, pp. 119–153.

[19]Acton, E., "A Modelling of Large Eddies in an Axisymmetric Jet," *Journal of Fluid Mechanics*, Vol. 98, Pt. 1, 1980, pp. 1–31.

[20]Mook, D. T., Roy, S., Choksi, G., and Dong, B., "Numerical Simulation of the Unsteady Wake Behind an Airfoil," *Journal of Aircraft*, Vol. 26, No. 6, 1989, pp. 509–514.

[21]Townsend, A. A., *The Structure of Turbulent Shear Flow*, 2nd ed., Cambridge Univ. Press, Cambridge, England, UK, 1976.

[22]Yu, M.-H., and Monkewitz, P. A., "Oscillations in the Near Field of a Heated Two-Dimensional Jet," *Journal of Fluid Mechanics*, Vol. 255, 1993, pp. 323–347.

[23]Monkewitz, P. A., Bechert, D. W., Barsikow, B., and Lehmann, B., "Self-Excited Oscillations and Mixing in a Heated Round Jet," *Journal of Fluid Mechanics*, Vol. 213, 1990, pp. 611–639.

[24]Jumper, E. J., Hugo, R. J., and Cicchiello, J. M., "Turbulent-Fluid-Induced Optical Wavefront Dynamics: Near- and Far-Field Implications," AIAA Paper 94-2547, June 1994.

[25]Hugo, R. J., and Jumper, E. J., "Experimental Measurement of a Time-Varying Optical Path Difference Using the Small-Aperture Beam Technique," *Optical Diagnostics in Fluid and Thermal Flow*, edited by S. S. Cha and J. D. Trolinger, Vol. 2005, SPIE—International Society of Optical Engineering, Bellingham, WA, 1993, pp. 116–128.